CORRECTED 28 SEPTEMBER 2016; SEE FULL TEXT

RESEARCH ARTICLE

STRUCTURAL BIOLOGY

The apo-structure of the leucine sensor Sestrin2 is still elusive

Robert A. Saxton,[1,2,3,4,5] Kevin E. Knockenhauer,[1]* Thomas U. Schwartz,[1]† David M. Sabatini[1,2,3,4,5]†

Sestrin2 is a GATOR2-interacting protein that directly binds leucine and is required for the inhibition of mTORC1 under leucine deprivation, indicating that it is a leucine sensor for the mTORC1 pathway. We recently reported the structure of Sestrin2 in complex with leucine [Protein Data Bank (PDB) ID, 5DJ4] and demonstrated that mutations in the leucine-binding pocket that alter the affinity of Sestrin2 for leucine result in a corresponding change in the leucine sensitivity of mTORC1 in cells. A lower resolution structure of human Sestrin2 (PDB ID, 5CUF), which was crystallized in the absence of exogenous leucine, showed Sestrin2 to be in a nearly identical conformation as the leucine-bound structure. On the basis of this observation, it has been argued that leucine binding does not affect the conformation of Sestrin2 and that Sestrin2 may not be a sensor for leucine. We show that simple analysis of the reported "apo"-Sestrin2 structure reveals the clear presence of prominent, unmodeled electron density in the leucine-binding pocket that exactly accommodates the leucine observed in the higher resolution structure. Refining the reported apo-structure with leucine eliminated the large F_{obs}-F_{calc} difference density at this position and improved the working and free R factors of the model. Consistent with this result, our own structure of Sestrin2 crystallized in the absence of exogenous leucine also contained electron density that is best explained by leucine. Thus, the structure of apo-Sestrin2 remains elusive.

INTRODUCTION

The mechanistic target of rapamycin complex 1 (mTORC1) couples cell growth with the availability of biosynthetic inputs such as amino acids (*1*, *2*). Leucine, in particular, robustly activates mTORC1, and leucine deprivation inhibits mTORC1 signaling in a wide variety of experimental systems (*3*–*5*). Recently, we identified Sestrin2 as a key leucine sensor in mammalian cells (*6*, *7*). Leucine binds directly to Sestrin2 in vitro, and genetic loss of Sestrin2 and its closely related homologs renders mTORC1 signaling resistant to inhibition by leucine starvation. Mechanistically, Sestrin2 inhibits mTORC1 in the absence of leucine by binding to GATOR2, an upstream activator of mTORC1 (*7*–*9*). The addition of leucine triggers the dissociation of Sestrin2 from GATOR2 both in vitro and in cells, suggesting that leucine binding induces a conformational change in Sestrin2 that disrupts this interaction (*6*, *7*). Consistent with this, leucine substantially increases the thermal stability of purified Sestrin2, as is often observed for ligand-receptor complexes (*6*, *7*, *10*).

We solved the crystal structure of human Sestrin2 in complex with leucine at a 2.7 Å resolution, revealing insights into the mechanism of leucine sensing (*6*). However, Sestrin2 failed to crystallize in the absence of leucine, and the structure of apo-Sestrin2 remained elusive. Subsequently, a 3.5 Å structure of Sestrin2 that crystallized without the addition of exogenous leucine was reported, in the same crystal form, showing Sestrin2 in a nearly identical conformation as the leucine-bound structure (*11*). On the basis of this observation, Lee *et al*. argued that the similarities between the reported "apo"-structure (*11*) of Sestrin2 and the leucine-bound structure (*6*) are inconsistent with Sestrin2 being a sensor for leucine (*12*, *13*).

To reconcile our structural, biochemical, and cell biological data with the claims made by Lee *et al*. (*12*), we reanalyzed their reported apo-Sestrin2 structure [Protein Data Bank (PDB) ID, 5CUF], revealing the clear presence of a ligand bound in the leucine-binding pocket. In addition, we report our own 3.0 Å structure of Sestrin2 that we obtained without adding exogenous leucine during the purification process, in which leucine is also present.

RESULTS

Using the corresponding structure factors and atomic model deposited in the PDB, we calculated the $2F_{obs}$-F_{calc} and F_{obs}-F_{calc} electron density maps for the protein with PDB ID 5CUF. Simple inspection of the F_{obs}-F_{calc} difference map, which highlights discrepancies between experimental data and the structural model, revealed the presence of substantial unexplained electron density (positive 7.5σ peak) at the exact location of the leucine-binding pocket observed in the leucine-bound Sestrin2 (PDB ID, 5DJ4; Fig. 1A). This unmodeled density is easily observed in all five crystallographically independent copies of Sestrin2 in the asymmetric unit and is the prime location where modeled density and observed density differ. Furthermore, the unexplained electron density in 5CUF resembles the density corresponding to leucine in the higher-resolution 5DJ4 structure (Fig. 1B). To test whether this density may represent leucine, we refined the 5CUF model either with or without leucine built into it. As with 5DJ4, refining 5CUF with leucine eliminated the F_{obs}-F_{calc} map peak at the binding site and improved the *R*-factors of the model (Fig. 1, B, C, and E), consistent with the presence of bound leucine in this structure.

We also analyzed the possibility that one of the buffer components (MES, tris, sodium, chloride, malonate, and TCEP) of the reported crystallization condition of 5CUF may be contributing to the large difference density at the leucine-binding site (*11*). The only ingredient that could be reasonably considered at the modest resolution of 3.5 Å as a leucine substitute is malonate (Fig. 1D). It is the main precipitant at a 1.15 M concentration, and it could at least mimic the interaction of the carboxyl group of leucine. However, the contacts formed by the hydrophobic leucine side chain, as well as by the cationic amine group, would still be unexplained. Nonetheless, refining 5CUF

[1]Department of Biology, Massachusetts Institute of Technology, Cambridge, MA 02139, USA. [2]Whitehead Institute for Biomedical Research, 9 Cambridge Center, Cambridge, MA 02142, USA. [3]Howard Hughes Medical Institute, Cambridge, MA 02139, USA. [4]Koch Institute for Integrative Cancer Research, 77 Massachusetts Avenue, Cambridge, MA 02139, USA. [5]Broad Institute of Harvard and Massachusetts Institute of Technology, 415 Main Street, Cambridge, MA 02142, USA.
*Present address: Novartis Institutes for BioMedical Research, 250 Massachusetts Avenue, Cambridge, MA 02139, USA.
†Corresponding author. Email: sabatini@wi.mit.edu (D.M.S.); tus@mit.edu (T.U.S.)

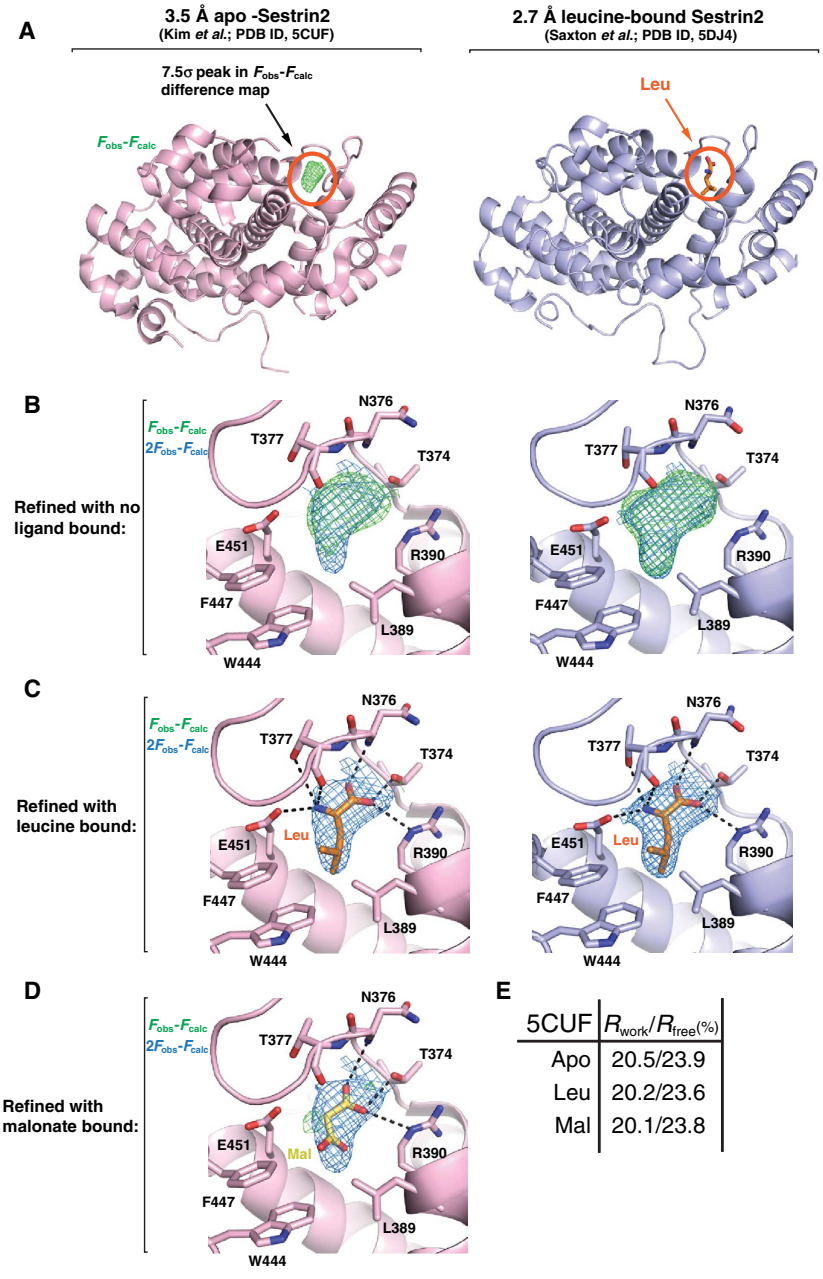

Fig. 1. Identification of ligand in the apo-Sestrin2 structure reported by Kim *et al.* (*11*). (**A**) Ribbon diagrams of the reported apo-Sestrin2 structure (5CUF; pink, left) and the leucine-bound structure (5DJ4; light blue, right). The largest peak in the 3.5 Å 5CUF F_{obs}-F_{calc} difference map, contoured at 3σ, is shown as a green mesh in the 5CUF structure. The bound leucine built into the 5DJ4 structure is shown in orange. (**B**) Close-up view of the leucine-binding pocket of Sestrin2 in the 3.5 Å 5CUF (left) and the 2.7 Å 5DJ4 structures (right), refined without leucine built into the model. The F_{obs}-F_{calc} (green mesh) and $2F_{obs}$-F_{calc} (blue mesh) electron density maps were contoured at 3σ and 1σ, respectively, and shown in the location of the bound leucine. (**C**) The 5CUF and 5DJ4 structures were refined with leucine built into the model and shown in the same view as in (B). The F_{obs}-F_{calc} and $2F_{obs}$-F_{calc} electron density maps are depicted as in (B). Hydrogen bonds and electrostatic interactions are shown as black dashed lines. (**D**) The 5CUF structure was refined with malonate built into the model and shown in the same view as in (B). The F_{obs}-F_{calc} and $2F_{obs}$-F_{calc} electron density maps are depicted as in (B). (**E**) The R_{work}/R_{free} (%) for the 5CUF structure refined with no ligand, leucine, or malonate modeled.

5CUF	R_{work}/R_{free}(%)
Apo	20.5/23.9
Leu	20.2/23.6
Mal	20.1/23.8

with malonate also eliminated the F_{obs}-F_{calc} map peak and improved the *R*-factors of the model (Fig. 1, D and E).

In our own efforts to obtain the structure of apo-Sestrin2, we purified Sestrin2 from *Escherichia coli* and crystallized it without the addition of leucine after bacterial cell lysis. Whereas preincubating Sestrin2 with leucine yielded large, high-quality crystals within 24 to 48 hours of setting drops, the crystals that formed in the absence of added leucine were smaller, took much longer to crystallize (7 to 14 days), and formed in a background of a heavy protein precipitate. Nonetheless, we obtained high-quality crystals from which we obtained a structure at a 3.0 Å resolution (PDB ID, 5T0N; Table 1). Inspection of the F_{obs}-F_{calc} difference map for this structure again revealed a large positive peak in the location of the leucine-binding pocket that strongly resembles the electron density of leucine (Fig. 2A). As with 5CUF and 5DJ4, refining the structure with leucine eliminated the F_{obs}-F_{calc} peak and improved the model statistics (Fig. 2, B and D). Furthermore, at this resolution, leucine is clearly the best candidate to fit into this density because malonate does not fully explain the difference density at this position and did not improve the *R*-factors as substantially as when the structure was refined with leucine (Fig. 2, C and D).

DISCUSSION

The leucine-binding site of Sestrin2 consists of a shallow hydrophobic pocket flanked on each side by opposing positive and negative charges contributed by Arg^{390} and Glu^{451}, respectively, making it well suited to specifically accommodate zwitterionic α-amino acids with short aliphatic side chains (*6*). Among the amino acids, Sestrin2 has the highest affinity for leucine, with about 15- and 30-fold lower affinity for the closely related amino acids methionine and isoleucine, respectively, and undetectable affinity for the remaining natural amino acids (*7*). In addition, whereas it is impossible to definitively conclude whether the density present in the 3.5 Å 5CUF structure corresponds to leucine or another ligand such as malonate, our own 3.0 Å structure clearly favors leucine as the best candidate to explain the observed density. In any case, these data conclusively demonstrate that 5CUF represents a ligand-bound form of Sestrin2, not the apo-Sestrin2 conformation as reported by Lee *et al.* (*12*) based on the data in Kim *et al.* (*11*).

Although leucine is highly abundant in bacterial cells (*14*), it may seem surprising that Sestrin2 can remain stably bound to leucine throughout the purification process given the reported 20 μM affinity of Sestrin2 for leucine (*7*). One possibility is that the off-rate of the Sestrin2-leucine interaction is substantially lower in the absence of additional protein components or

Table 1. Data collection and refinement statistics. RMS, root mean square. Values in parentheses are those for the highest resolution shell.

Protein	"Pseudo-apo"–Sestrin2
Organism	*Homo sapiens*
PDB ID	5T0N
Data collection	
Space group	I23
a, *b*, and *c* (Å)	292.26, 292.26, and 292.26
α, β, and γ (°)	90.0, 90.0, and 90.0
Wavelength (Å)	0.9792
Resolution range (Å)	200.0–3.0 (3.05–3.00)
Completeness (%)	100 (100)
Redundancy	40.7 (41.9)
R_{meas} (%)	28.0 (>100)
R_{pim} (%)	4.4 (37.8)
I/σ	19.5 (2.0)
Refinement	
Resolution range (Å)	103.3–3.0
R_{work} (%)	18.9
R_{free} (%)	22.5
Number of reflections	
Total	82,205
R_{free} reflections	1,637
Number of nonhydrogen atoms	14,648
Protein atoms	14,648
RMS deviations	
Bond lengths (Å)	0.010
Bond angles (°)	1.037
Average *B*-factor (Å^2)	
Protein	49.0
Ramachandran (%)	
Favored	96.4
Allowed	3.0
Outlier	0.7

posttranslational modifications present only in mammalian cells, such that a small fraction of Sestrin2 remains bound to leucine even after purification. Crystallization is, after all, a purification method and is thus perfectly suited to enrich a small fraction of leucine-bound Sestrin2 in a large background of noncrystallizing apo-Sestrin. Because all three Sestrin2 crystal structures crystallize under highly similar conditions and in the same crystal form and because the largest and best diffracting crystals grow in the presence of leucine, we conclude that all reported structures are best interpreted as bound to leucine.

In summary, we argue that the 5CUF structure depicts Sestrin2 in the ligand-bound conformation, not the apo-conformation as reported by Lee *et al.* (*12*). The leucine-dependent dissociation of Sestrin2 from GATOR2 represents the critical first step in the activation of mTORC1 by leucine and understanding how leucine-binding alters the conformation of Sestrin2 to disrupt its interaction with GATOR2 remains a major open question in the field.

MATERIALS AND METHODS

Protein production and purification

Human Sestrin2 was expressed and purified as described previously (*6*). Briefly, full-length, codon-optimized human Sestrin2 was N-terminally fused with a human rhinovirus 3C protease–cleavable His^{10}-Arg^{8}-ScSUMO tag and cloned into a pETDuet-1 bacterial expression vector. This vector was transformed into *E. coli* LOBSTR (DE3) cells (Kerafast) (*15*). Cells were grown at 37°C to 0.6 optical density, then protein production was induced with 0.2 mM isopropyl-β-D-thiogalactopyranoside at 18°C for 12 to 14 hours. Cells were collected by centrifugation at 6000*g*, resuspended in lysis buffer [50 mM potassium phosphate (pH 8.0), 500 mM NaCl, 30 mM imidazole, 3 mM β-mercaptoethanol (βME), and 1 mM phenylmethylsulfonyl fluoride], and lysed with a cell disruptor (Constant Systems). The lysate was cleared by centrifugation at 10,000*g* for 20 min. The soluble fraction was incubated with Ni-Sepharose 6 Fast Flow beads (GE Healthcare) for 30 min

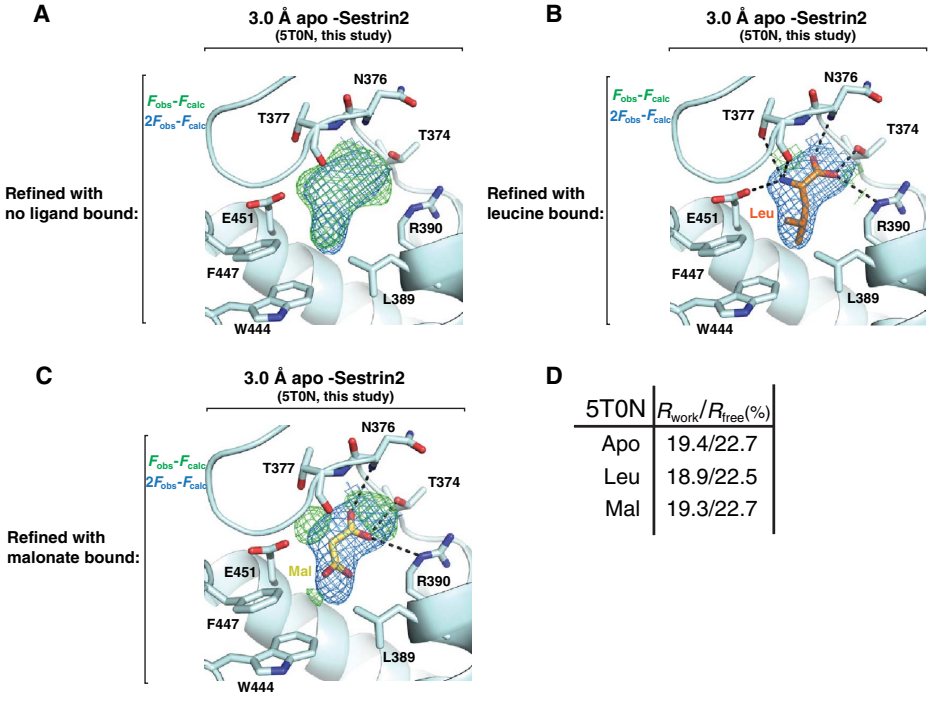

5T0N	R_{work}/R_{free}(%)
Apo	19.4/22.7
Leu	18.9/22.5
Mal	19.3/22.7

Fig. 2. Sestrin2 crystallizes in complex with leucine without the addition of exogenous leucine. (A) Close-up view of the leucine-binding pocket in Sestrin2 (5T0N; this study) refined without leucine built into the model. The F_{obs}-F_{calc} (green mesh) and $2F_{obs}$-F_{calc} (blue mesh) electron density maps, contoured at 3σ and 1σ, respectively, are shown as in Fig. 1B. (B) Close-up view of the leucine-binding pocket in Sestrin2 refined with leucine built into the model. The F_{obs}-F_{calc} and $2F_{obs}$-F_{calc} electron density maps are depicted as in (A). Hydrogen bonds and electrostatic interactions are shown as black dashed lines. (C) Close-up view of the leucine-binding pocket in Sestrin2 refined with malonate built into the model. The F_{obs}-F_{calc} and $2F_{obs}$-F_{calc} electron density maps are depicted as in (A). Hydrogen bonds and electrostatic interactions are shown as black dashed lines. (D) The R_{work}/R_{free} (%) for the 5T0N structure (this study) refined with no ligand, leucine, or malonate modeled.

on ice. After washing the beads with lysis buffer, the protein was eluted in 250 mM imidazole (pH 8.0), 150 mM NaCl, and 3 mM βME. The Ni eluate was diluted at a 1:1 ratio with 10 mM potassium phosphate (pH 8.0), 0.1 mM EDTA, and 1 mM dithiothreitol (DTT) and was subjected to cation-exchange chromatography on a 5-ml SP Sepharose fast flow column (GE Healthcare) with a linear NaCl gradient. The eluted Sestrin2 was then incubated with 3C protease and dialyzed overnight at 4°C into 10 mM potassium phosphate (pH 8.0), 150 mM NaCl, 0.1 mM EDTA, and 1 mM DTT, followed by a second cation-exchange chromatography run on an SP Sepharose fast flow column (GE Healthcare) with a linear NaCl gradient. The protein was further purified by size-exclusion chromatography on a Superdex S200 16/60 column (GE Healthcare) equilibrated in running buffer [10 mM tris-HCl (pH 8.0), 150 mM NaCl, 0.1 mM EDTA, and 1 mM DTT].

Crystallization conditions

Crystals were grown at 18°C by hanging drop vapor diffusion with 1 μl of Sestrin2 (5 mg/ml) mixed with an equal volume of reservoir solution containing 100 mM MES (pH 6.0), 1.2 M disodium malonate, and 1% (v/v) Jeffamine ED-2001. Drops were microseeded to obtain well-diffracting crystals. Microseeds were obtained as described previously (*16*). Briefly, a single 2-μl drop containing crystals of Sestrin2 was diluted into a 50-μl solution of mother liquor [100 mM MES (pH 6.0), 1.2 M disodium malonate, and 1% (v/v) Jeffamine ED-2001], vortexed for 5 min in the presence of a polystyrene bead, then diluted again into 500 μl of mother liquor. This solution was then diluted at a ratio of 1:1000 to obtain the final microseed stock. Microseed stock (0.2 μl) was then added to the 2-μl hanging drop described above (for a final total dilution of 1:2,500,000). Crystals were cryoprotected in mother liquor supplemented with 18% (v/v) glycerol.

Data collection and structure determination

Data collection was performed at the Advanced Photon Source end station 24-IDC at the Argonne National Laboratory. All data processing steps were carried out with programs provided through SBGrid (*17*). Data reduction was performed with HKL-2000 (*18*). The phase problem was solved by molecular replacement using our published Sestrin2 structure (5DJ4) as the search model in the Phaser-MR program, run as part of the Phenix Autosol program (space group I23; five molecules per asymmetric unit) (*19*). To reduce potential model bias, we used a search model lacking the bound leucine and surrounding protein residues. An interpretable 3.0 Å electron density map was obtained, and model building was carried out in Coot (*20*). Subsequent refinement was carried out using phenix.refine.

Structure and electron density map analysis

For analysis of published structures 5DJ4 and 5CUF, the F_{obs}-F_{calc} and $2F_{obs}$-F_{calc} maps were calculated from the models and structure factors deposited in the PDB using phenix.maps and visualized in Coot (*20*). Refinement of the models either with or without bound leucine or malonate built in was performed using phenix.refine. *xyz* coordinates and individual *B*-factors were refined over three cycles. All structure figures were made in PyMOL (*21*).

REFERENCES AND NOTES

1. C. C. Dibble, B. D. Manning, Signal integration by mTORC1 coordinates nutrient input with biosynthetic output. *Nat. Cell Biol.* **15**, 555–564 (2013).
2. M. Laplante, D. M. Sabatini, mTOR signaling in growth control and disease. *Cell* **149**, 274–293 (2012).
3. C. J. Lynch, H. L. Fox, T. C. Vary, L. S. Jefferson, S. R. Kimball, Regulation of amino acid–sensitive TOR signaling by leucine analogues in adipocytes. *J. Cell. Biochem.* **77**, 234–251 (2000).
4. J. C. Anthony, F. Yoshizawa, T. G. Anthony, T. C. Vary, L. S. Jefferson, S. R. Kimball, Leucine stimulates translation initiation in skeletal muscle of postabsorptive rats via a rapamycin-sensitive pathway. *J. Nutr.* **130**, 2413–2419 (2000).
5. D.-H. Kim, D. D. Sarbassov, S. M. Ali, J. E. King, R. R. Latek, H. Erdjument-Bromage, P. Tempst, D. M. Sabatini, mTOR interacts with raptor to form a nutrient-sensitive complex that signals to the growth machinery. *Cell* **110**, 163–175 (2002).
6. R. A. Saxton, K. E. Knockenhauer, R. L. Wolfson, L. Chantranupong, M. E. Pacold, T. Wang, T. U. Schwartz, D. M. Sabatin, Structural basis for leucine sensing by the Sestrin2-mTORC1 pathway. *Science* **351**, 53–58 (2016).
7. R. L. Wolfson, L. Chantranupong, R. A. Saxton, K. Shen, S. M. Scaria, J. R. Cantor, D. M. Sabatini, Sestrin2 is a leucine sensor for the mTORC1 pathway. *Science* **351**, 43–48 (2016).
8. L. Chantranupong, R. L. Wolfson, J. M. Orozco, R. A. Saxton, S. M. Scaria, L. Bar-Peled, E. Spooner, M. Isasa, S. P. Gygi, D. M. Sabatini, The sestrins interact with GATOR2 to negatively regulate the amino-acid-sensing pathway upstream of mTORC1. *Cell Rep.* **9**, 1–8 (2014).
9. A. Parmigiani, A. Nourbakhsh, B. Ding, W. Wang, Y. C. Kim, K. Akopiants, K.-L. Guan, M. Karin, A. V. Budanov, Sestrins inhibit mTORC1 kinase activation through the GATOR complex. *Cell Rep.* **9**, 1281–1291 (2014).
10. F. H. Niesen, H. Berglund, M. Vedadi, The use of differential scanning fluorimetry to detect ligand interactions that promote protein stability. *Nat. Protoc.* **2**, 2212–2221 (2007).
11. H. Kim, S. An, S.-H. Ro, F. Teixeira, G. J. Park, C. Kim, C.-S. Cho, J.-S. Kim, U. Jakob, J. H. Lee, U.-S. Cho, Janus-faced Sestrin2 controls ROS and mTOR signalling through two separate functional domains. *Nat. Commun.* **6**, 10025 (2015).
12. J. H. Lee, U.-S. Cho, M. Karin, Sestrin regulation of TORC1: Is Sestrin a leucine sensor? *Sci. Signal.* **9**, re5 (2016).
13. A. Ho, C.-S. Cho, S. Namkoong, U.-S. Cho, J. H. Lee, Biochemical basis of sestrin physiological activities. *Trends Biochem. Sci.* **41**, 621–632 (2016).
14. T. Sajed, A. Marcu, M. Ramirez, A. Pon, A. C. Guo, C. Knox, M. Wilson, J. R. Grant, Y. Djoumbou, D. S. Wishart, ECMDB 2.0: A richer resource for understanding the biochemistry of *E. coli*. *Nucleic Acids Res.* **44**, D495–D501 (2015).
15. K. R. Andersen, N. C. Leksa, T. U. Schwartz, Optimized *E. coli* expression strain LOBSTR eliminates common contaminants from His-tag purification. *Proteins* **81**, 1857–1861 (2013).
16. J. R. Luft, G. T. DeTitta, A method to produce microseed stock for use in the crystallization of biological macromolecules. *Acta Cryst.* **D55**, 988–993 (1999).
17. A. Morin, B. Eisenbraun, J. Key, P. C. Sanschagrin, M. A. Timony, M. Ottaviano, P. Sliz, Collaboration gets the most out of software. *Elife* **2**, e01456 (2013).
18. Z. Otwinowski, W. Minor, Processing of X-ray diffraction data collected in oscillation mode. *Methods Enzymol.* **276**, 307–326 (1997).
19. P. D. Adams, P. V. Afonine, G. Bunkóczi, V. B. Chen, I. W. Davis, N. Echols, J. J. Headd, L.-W. Hung, G. J. Kapral, R. W. Grosse-Kunstleve, A. J. McCoy, N. W. Moriarty, R. Oeffner, R. J. Read, D. C. Richardson, J. S. Richardson, T. C. Terwilliger, P. H. Zwart, *PHENIX*: A comprehensive Python-based system for macromolecular structure solution. *Acta Crystallogr. D Biol. Crystallogr.* **D66**, 213–221 (2010).
20. P. Emsley, B. Lohkamp, W. G. Scott, K. Cowtan, Features and development of *Coot*. *Acta Crystallogr. D Biol. Crystallogr.* **D66**, 486–501 (2010).
21. L. L. C. Schrödinger, The PyMOL Molecular Graphics System, version 1.3r1 (2010).

Acknowledgments: We thank all members of the Sabatini and Schwartz Laboratories for helpful insights. **Funding:** This work is based on a research conducted at the Northeastern Collaborative Access Team beamlines, which are funded by the National Institute of General Medical Sciences of the NIH (P41 GM103403). The Pilatus-6M detector on 24-IDC beamline is funded by an NIH Office of Research Infrastructure Programs High-End Instrumentation grant (S10 RR029205). This research used resources of the Advanced Photon Source, a U.S. Department of Energy (DOE) Office of Science user facility operated for the DOE Office of Science by Argonne National Laboratory under contract no. DE-AC02-06CH11357. This work was supported by grants from the NIH (R01CA103866 and AI47389) and the U.S. Department of Defense (W81XWH-07- 0448) to D.M.S. D.M.S. is an investigator of the Howard Hughes Medical Institute. **Author contributions:** R.A.S., T.U.S., and D.M.S. designed the research plan. R.A.S. performed the crystallographic experiments with input from K.E.K. and T.U.S. R.A.S., K.E.K., and T.U.S. analyzed the structural data. R.A.S., T.U.S., and D.M.S. wrote and all authors edited the manuscript. **Competing interests:** D.M.S. is a founder and a member of the Scientific Advisory Board, a paid consultant, and a shareholder of Navitor Pharmaceuticals, which targets for therapeutic benefit of the amino acid sensing pathway upstream of mTORC1. The other authors declare that they have no competing interests. **Data and materials availability:** Coordinates and structure factors for the x-ray crystal structure of the pseudo-apo–Sestrin2 have been deposited in the PDB with accession code 5T0N.

Submitted 28 June 2016
Accepted 25 August 2016
Final Publication 20 September 2016
10.1126/scisignal.aah4497
Citation: R. A. Saxton, K. E. Knockenhauer, T. U. Schwartz, D. M. Sabatini, The apo-structure of the leucine sensor Sestrin2 is still elusive. *Sci. Signal.* **9**, ra92 (2016).

The apo-structure of the leucine sensor Sestrin2 is still elusive
Robert A. Saxton, Kevin E. Knockenhauer, Thomas U. Schwartz and David M. Sabatini (September 20, 2016)
Science Signaling **9** (446), ra92. [doi: 10.1126/scisignal.aah4497]